

<https://doi.org/10.15407/scine20.03.053>

RUSANOV, A. V.<sup>1</sup> (<https://orcid.org/0000-0002-9957-8974>),  
 SUBOTIN, V. H.<sup>2</sup> (<https://orcid.org/0000-0002-2489-5836>),  
 KHORYEV, O. M.<sup>1</sup> (<https://orcid.org/0000-0001-6940-4183>),  
 LYNNYK, O. V.<sup>2</sup> (<https://orcid.org/0000-0003-1946-3032>),  
 BYKOV, Yu. A.<sup>1</sup> (<https://orcid.org/0000-0001-7089-8993>),  
 KOROTAIEV, P. O.<sup>1</sup> (<https://orcid.org/0000-0002-7473-9508>),  
 and AHIBALOV, Ye. S.<sup>1</sup> (<https://orcid.org/0000-0003-3866-9992>)

<sup>1</sup> Anatolii Pidhornyi Institute of Mechanical Engineering Problems  
 of National Academy of Sciences of Ukraine,  
 2/10, Pozharskyi St., Kharkiv, 61046, Ukraine,  
 +380 57 349 4724, [admi@ipmach.kharkov.ua](mailto:admi@ipmach.kharkov.ua)

<sup>2</sup> JSC Ukrainian Energy Machines,  
 199, Heroiv Kharkova Ave., Kharkiv, 61037, Ukraine,  
 +380 57 349 2171, [office@ukrenergymachines.com](mailto:office@ukrenergymachines.com)

## EXPERIMENTAL STUDIES OF PRESSURE PULSATIONS IN DRAFT TUBE DIFFUSER OF PUMP-TURBINE MODELS FOR HEADS UP TO 200 m

**Introduction.** Increasing the share of balancing capacities to cover daily peaks in electricity consumption is one of the top priorities of the postwar development of Ukraine's energy sector.

**Problem Statement.** Today, power plant hydraulic turbines need both to increase efficiency and to expand their operating range. For example, the new hydraulic units of the Dniester PSP shall operate in turbine mode in the range of 40–100% of rated capacity, while the four previous units operate in the range of 70–100%. This requirement can be met by increasing efficiency and reducing pulsations at low power output.

**Purpose.** Based on studying the influence of blade spatial shape of a Francis pump-turbine runners on flow part hydrodynamics, to identify the patterns of pressure fluctuations distribution in draft tube diffuser of the hydraulic unit model.

**Materials and Methods.** Three options of models (the original and two modified ones) have been studied on the IMEP ECS-30 hydrodynamic test stand. The runner blades are made of PLA plastic by 3D printing. Pressure pulsations are measured by sensors at two points of draft tube diffuser at a distance of 0.2 and 1.5 runner diameters from the runner bottom shroud.

**Results.** Three modifications of the pump-turbine runner for heads up to 200 m have been designed and experimentally studied with the use of circumferential lean that differ from the original version only in relative position of blade profiles. The analysis of obtained energy and pulsation characteristics of the models in turbine mode has shown that the model with the runner having a negative circular blade lean has the best performance.

Citation: Rusanov, A. V., Subotin, V. H., Khoryev, O. M., Lynnyk, O. V., Bykov, Yu. A., Korotaiev, P. O., and Ahibalov, Ye. S. (2024). Experimental Studies of Pressure Pulsations in Draft Tube Diffuser of Pump-Turbine Models for Heads up to 200 m. *Sci. innov.*, 20(3), 53–66. <https://doi.org/10.15407/scine20.03.053>

© Publisher PH “Akademiya” of the NAS of Ukraine, 2024. This is an open access article under the CC BY-NC-ND license (<https://creativecommons.org/licenses/by-nc-nd/4.0/>)

**Conclusions.** The determined influence of spatial shape of the runner blades on the energy and pulsation characteristics of the Francis pump-turbine model for heads up to 200 m has made it possible to increase its efficiency and to reduce the level of pressure fluctuations in the flow part.

**Keywords:** pump-turbine, flow part, pressure pulsations, runner, draft tube, and experimental studies.

## Nomenclature

$D_1$	— model runner diameter, m
$\eta^*$	— relative efficiency, %
$n'_1$	— unit speed of rotation, $\text{min}^{-1}$
$Q'_1$	— unit discharge, $\text{m}^3/\text{s}$
$N'_1$	— unit power, kW
$rms$	— standard deviation of pressure fluctuations
$H$	— head, m
$a_0$	— guide vane opening, mm

## Subscripts

P	— pump mode
T	— turbine mode
max	— maximum value

## Abbreviations

PSP	— pumped storage plant
IMEP	— Institute of Mechanical Engineering Problems
HPP	— hydroelectric power plant

According to the report of the International Renewable Energy Agency (IRENA), in order to meet the targets, set out in the Paris Climate Agreement, the world needs to more than double its hydropower capacity, including the capacity of pumped storage facilities, by 2050 [1]. To achieve this goal, annual investments in hydropower should increase 5 times and amount to approximately USD 85 billion in conventional hydropower and USD 8.8 billion in pumped storage [1]. The majority of hydropower capacity is located in Asia, accounting for 42 percent, followed by Europe, North America, South America, and the rest of the world. Over the past decade, investment in hydropower has been lower than in solar and wind power, despite being one of the cheapest and most stable sources of renewable energy.

Ukraine's hydropower industry is based on cascades of hydroelectric power plants on the Dnipro

and Dniester rivers, as well as the Dniester, Kyiv, and Tashlyk PSPs. The priority in the postwar development of hydropower is to fully restore the generation volumes accounted for by balancing capacities, as well as to complete 5–7 hydroelectric units at Dniester, after which this plant will become the most powerful in Europe.

Today, when designing hydraulic machines, including pump-turbines at PSPs, there are requirements not only to increase efficiency and improve cavitation characteristics [2], but also to expand the range of operation in turbine mode to the partial load zone [3]. For example, the new hydraulic units of the Dniester PSPP with station numbers 5–7 shall operate reliably in the range of 40–100% of their rated capacity, while the four previously installed units have never been operated at capacities below 70%.

One of the important reasons for the prohibition of partial load operation is the formation of a vortex rope in the draft tube [4], the precession of which can lead to vibrations of the entire unit [5]. The precession of the rope causes quite powerful periodic pressure pulsations that can spread to the entire flow part [6]. The precession frequency of the vortex rope is quite low and is in the same range as the natural frequencies of the structural elements of the hydraulic unit, which can cause resonant vibrations [7].

The study of unsteady phenomena in draft tubes and runners of hydraulic machines is carried out both by numerical methods and on experimental facilities [8, 9]. The data obtained at real hydropower facilities are of the greatest value [10], since they make it possible to adjust the parameters of both the numerical experiment and the experiment on reduced models of the hydraulic machine [11]. Due to the complexity and danger of conducting full-scale experiments, the most common practice

is to use hydrodynamic test stands to study models of flow parts [12]. The study of unsteady phenomena, in particular, the precession of the vortex rope, is carried out both at partial [13] and close to nominal modes [14] and with increased flow rates [15], at which additional cavitation phenomena arise [16]. Experiments have revealed the nonstationary effect of the rope precession on the flow in the turbine runner [17] and have recorded additional ultra-low pulsation frequencies [18]. Along with experimental studies, numerical experiments have been widely used [19, 20].

Reducing the level of pulsations at the design stage of hydraulic machines is a difficult task [21]. Over the years, a large number of methods and technologies have been developed to bring the pulsation level to safe values [22]. The most commonly used ones are the installation of fins in the diffuser of the draft tube [23] and grilles at the outlet of the runner [24], injection of an air jet [25, 26], and changing the geometric characteristics of the runner blade system [27, 28]. Among the latter, the method of lengthening the cone of the runner is widely used [29, 30]. The presence of splitters in the runner can also affect the level of pulsations in both turbine and pump modes [31]. In recent years, the method of forming the trailing edge of the runner blade has become widespread. This fact may significantly reduce the level of pulsations in the draft tube [32].

The purpose of this research is to determine the patterns of pressure fluctuations and study the effect of the spatial shape of the blades (“circumferential lean”) of the runner of a Francis pump-turbine on the amplitudes and frequencies of unsteady flow in the draft tube diffuser of a hydraulic unit model.

One of the ways to influence the energy and pulsation characteristics of pump-turbines is to spatially profile the blades of radial-axial runners using circumferential leans. The use of circumferential leans makes it possible to change the shape of the blade edges and the relative position of the blade profiles in the circumferential direction by shifting the blade hub profile in the direction of rotor rota-

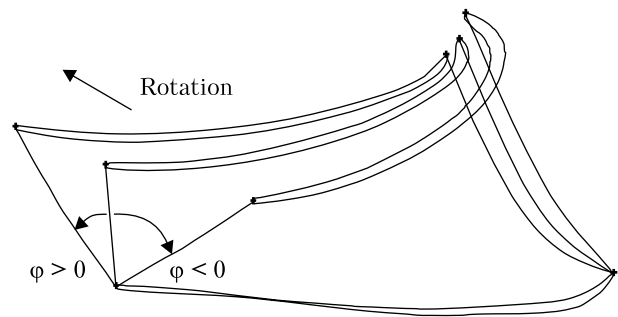


Fig. 1. Definition of the angle of the circumferential lean  $\varphi$

tion (positive lean, lean angle  $\varphi > 0$ ) or in the opposite direction (negative lean angle  $\varphi < 0$ ) (Fig. 1). At the same time, the shapes of the blade profiles remain unchanged. This approach makes it possible to optimize the blade shape to improve the fluid flow in the runner channel and in the draft tube.

The model of the Francis pump-turbine ORO5217, developed at IMEP and implemented at units 1–4 of the Dniester PSP, was taken as the initial object of study. The blades of the RK5217 runner have a traditional appearance: the trailing edge is located in the radial plane, the leading edge in the meridional projection is vertical and in the circumferential direction is inclined by  $10^\circ$  in the direction of rotor rotation.

Two modifications of the RK5217M and RK5217M2 runners were developed to study the effect of the blade spatial shape on the energy and pulsation characteristics using circumferential leans. In the RK5217M, the angle of inclination of the leading edge is  $\varphi = +45^\circ$ , respectively, the hub profile is shifted in the direction of rotor rotation by  $12.8^\circ$  relative to the original version, while the rest are linearly dependent on the height of the runner in the area of the leading edge. In RK5217M2, the angle of inclination of the leading edge is  $\varphi = -45^\circ$ , respectively, the hub profile is shifted by  $18.2^\circ$  in the direction opposite to the rotation relative to the original RK5217. Fig. 2 shows a computer model of the original and modified runner blades of the 5217 series.

At the first stage, using the *IPMFlow* software package [33] developed at IMEP, a numerical stu-

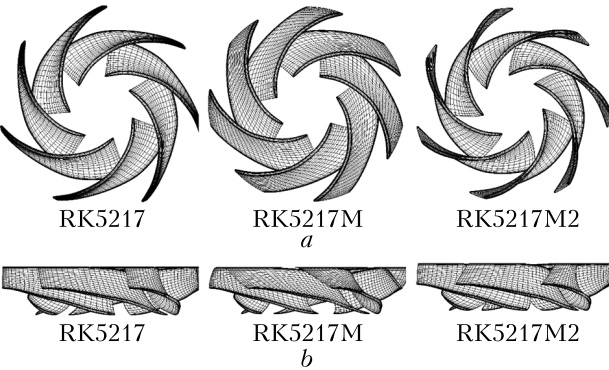


**Fig. 2.** Computer model of three options of runners: *a* – top view; *b* – front view

dy of the viscous flow of an incompressible fluid was carried out for three options of runners in a wide range of operation in turbine mode [34]. The *IPMFlow* software package allows for numerical studies in various flow parts [35, 36] using modern mathematical methods [37, 38]. The computational domain contained one channel each of the guide vane and the runner. The influence of the circumferential lean on the distribution of pressure and velocity vectors, pressure diagrams on the blades, the distribution of velocity components behind the runner, and the energy characteristics were analyzed. It was found that the best energy performance in almost the entire range of design modes is achieved by the RK5217M2 with a negative circumferential lean angle  $\varphi = -45^\circ$ .

**Table 1. Comparison of the Measurement Error of the Parameters of Model Hydraulic Turbines with the Requirements of IEC 60193**

Parameter	Measurement error	
	Requirements IEC 60193, %	Achieved value at the ECS-30 stand, %
Rotation speed	$\pm 0.075$	$\pm 0.030$
Head	$\pm 0.100$	$\pm 0.100$
Torque	$\pm 0.100$	$\pm 0.100$
Discharge	$\pm 0.200$	$\pm 0.200$
Model efficiency	$\pm 0.250$	$\pm 0.250$

Numerical studies of pressure pulsations in the diffuser of the draft tube for the RK5217 runner were also carried out by various turbulence models. Comparison of the calculation results with the known experimental data showed a satisfactory correspondence of the results [39].

To confirm the results of numerical studies and obtain reliable data in a wide range of turbine and pump modes, experimental selective tests of models with three options of runner with a diameter of  $D_1 = 350$  mm were carried out on the IMEP ECS-30 hydrodynamic test stand. The IMEP hydrodynamic stands have the status of national heritage and meet all the requirements of the international standard IEC 60193 for model acceptance tests of hydraulic machines of various types [40]. Table 1 shows a comparison of the measurement errors of parameters according to the requirements of IEC 60193 with the values achieved on the ECS-30 test stand.

The model unit of the pump-turbine consisted of a spiral casing with circular cross-sections and a  $360^\circ$  coverage angle, 20 stator columns, a guide vanes with 20 positive curvature blades and height of  $0.14D_1$ , a 7-blade runner, and a draft tube with a KU-3RO elbow. The runner blades were made of PLA plastic by 3D printing, which significantly reduced the cost and time of the research. Preliminary strength calculations of the blades showed the possibility of conducting experimental tests with heads up to 12 m. Figure 3 shows a photo of the 5217 series runners.

As a result of the energy studies, the operating and performance characteristics of the models with runners of the 5217 series were obtained.

Table 2 shows the parameters of the optimal modes of the three models of flow parts in the turbine and pump modes. The relative efficiency  $\eta^*$  in this paper is the ratio of the current efficiency value to its maximum value in the original version with the RK5217 runner. The results show that the maximum value of efficiency in both the turbine and pump modes in the model with the RK5217M2 runner with a negative lean  $\varphi = -45^\circ$  significantly exceeds the similar indicators of other

models. The position of the performance optima in the turbine mode changes insignificantly both in terms of flow rate and rotational speed. In the RK5217M2 model, the flow rate at the pump mode optimum is  $0.04 \text{ m}^3/\text{s}$  less than in the original version, which is also important because it requires less energy consumption when filling the upper reservoir. In addition, this runner has the lowest ratio of optimal rotational speeds in pump and turbine modes  $n'_{IP}/n'_{IT}$ , which confirms its advantages.

Table 3 shows the parameters of models with runners of the 5217 series at 50% and 95% of maximum capacity at maximum, nominal, and minimum heads at the Dniester PSP in turbine mode. From the presented results, it is clear that the model with RK5217M2 runner with a negative circumferential lean  $\varphi = -45^\circ$  has higher efficiency in almost the entire PSP operation range.

As can be seen, the use of spatial profiling of runner blades significantly affects the energy characteristics of the models both in the rated power operation zone ( $0.95 N'_{I\max}$ ) and in the partial load zone ( $0.50 N'_{I\max}$ ). As a result of the application



**Fig. 3.** Runners of the 5217 series, from left to right: RK5217M2, RK5217, RK5217M

of spatial profiling using leans in the RK5217M2 model ( $\varphi = -45^\circ$ ), it was possible to significantly improve the energy performance as compared with the modern high-performance RK5217, which successfully operated at hydraulic units 1–4 of the Dniester PSP.

Pulsation tests were performed to determine the amplitudes and frequencies of pressure pulsa-

**Table 2. Optimal Parameters of Flow Parts**

Runner	Turbine mode			Pump mode			$n'_{IP}/n'_{IT}$
	$Q'_I$	$n'_I$	$\eta^*$	$Q'_I$	$n'_I$	$\eta^*$	
RK5217	0.312	78.0	100.00	0.438	94.98	100.00	1.218
RK517M	0.317	76.0	98.52	0.348	96.18	98.73	1.266
RK5217M2	0.313	79.0	100.74	0.398	92.07	100.67	1.165

**Table 3. Energy Parameters of Models with Runner of the 5217 Series at 50% and 95% of the Maximum Capacity at Maximum, Nominal, and Minimum Heads at the Station in Turbine Mode**

Runner	At constant $N'_I = 0.50 \cdot N'_{I\max}$						At constant $N'_I = 0.95 \cdot N'_{I\max}$					
	$n'_I = 85$		$n'_I = 91$		$n'_I = 95$		$n'_I = 85$		$n'_I = 91$		$n'_I = 95$	
	$Q'_I$	$\eta^*$	$Q'_I$	$\eta^*$	$Q'_I$	$\eta^*$	$Q'_I$	$\eta^*$	$Q'_I$	$\eta^*$	$Q'_I$	$\eta^*$
RK5217	0.244	91.5	0.257	84.6	0.270	80.2	0.452	94.1	0.465	90.4	0.476	86.2
RK517M	0.246	89.3	0.253	85.3	0.253	81.7	0.458	91.0	0.470	87.4	0.482	84.0
RK5217M2	0.239	92.0	0.252	86.3	0.262	80.7	0.433	96.2	0.439	93.8	0.445	90.8

tions in the entire range of PSP operation modes. They were carried out at a head of  $H = 6$  m, which was accepted for power tests, in the flow part locations recommended by IEC 60193.

Pressure sensors of DMK331 type manufactured by BD SENSORS were used to measure pressure pulsations. The sensor membranes were installed flush with the surface of the flow part. The pulsations were measured at two points of the draft tube diffuser: the upper one at a distance of  $0.2D_1$  and the lower one at a distance of  $1.5D_1$  below the runner shroud (Fig. 4).

As secondary equipment, a special amplifier for measuring dynamic processes "Spider 8" manu-

factured by HBM (Germany) was used, followed by processing of the examined signal with the use of special program *Catman* on a personal computer and presenting the result in the form of an amplitude-frequency spectrum.

Graduation dependencies between the control pressure and instrument readings were determined by static calibration with the use of a load-piston manometer of the MP-6 type. The graduation dependence of the sensor is entered into the program settings to determine the value of the pressure pulsation amplitude.

The amplitudes of pressure fluctuations are presented as a dimensionless value in percent  $rms/H$ , where  $rms$  is the standard deviation of pressure fluctuations from the average value,  $H$  is the head during the test on the stand. The pressure pulsation frequencies are determined directly from the spectra obtained in the process of processing the test results at different operating modes of the pump-turbine models.

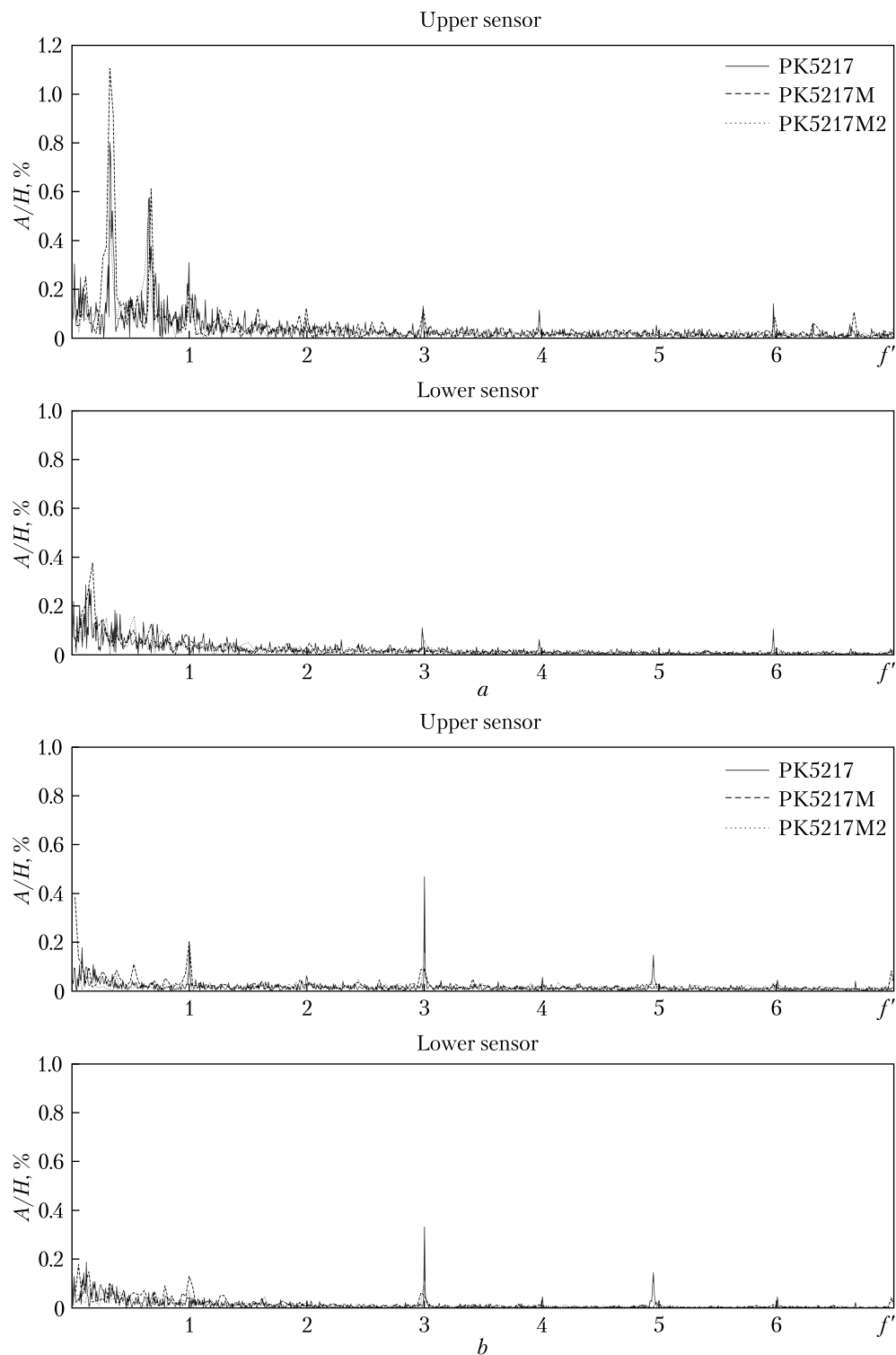
The study of pressure pulsations was carried out in the turbine mode at unit rotation speeds  $n'_1 = 85, 91, 95 \text{ min}^{-1}$ , corresponding to the maximum, nominal, and minimum heads of the Dniester PSP, in the range of unit discharge  $Q'_1$  from 0.100 to 0.450  $\text{m}^3/\text{s}$ , with guide vane openings  $a_0 = 8; 10; 12; 16; 20; 24; 28; 34 \text{ mm}$ . Based on the results of the study, the pulsation characteristics shown below were constructed.

Figure 5 shows the spectra of pressure pulsations in the draft tube diffuser obtained from the installed sensors (Fig. 4). The spectra are shown for three runners RK5217, RK5217M and RK5217M2 for the rotation speed  $n'_1 = 85 \text{ min}^{-1}$ , which corresponds to the maximum head, and two discharge values  $Q'_1 = 0.252$  and  $0.467 \text{ m}^3/\text{s}$ . The spectra are presented in dimensionless values, with the amplitude  $A/H$  and frequency  $f' = f / f_0$ , where  $f$  is the harmonic frequency,  $f_0$  is the rotation frequency,  $A$  is the pulsation amplitude, and  $H$  is the head.

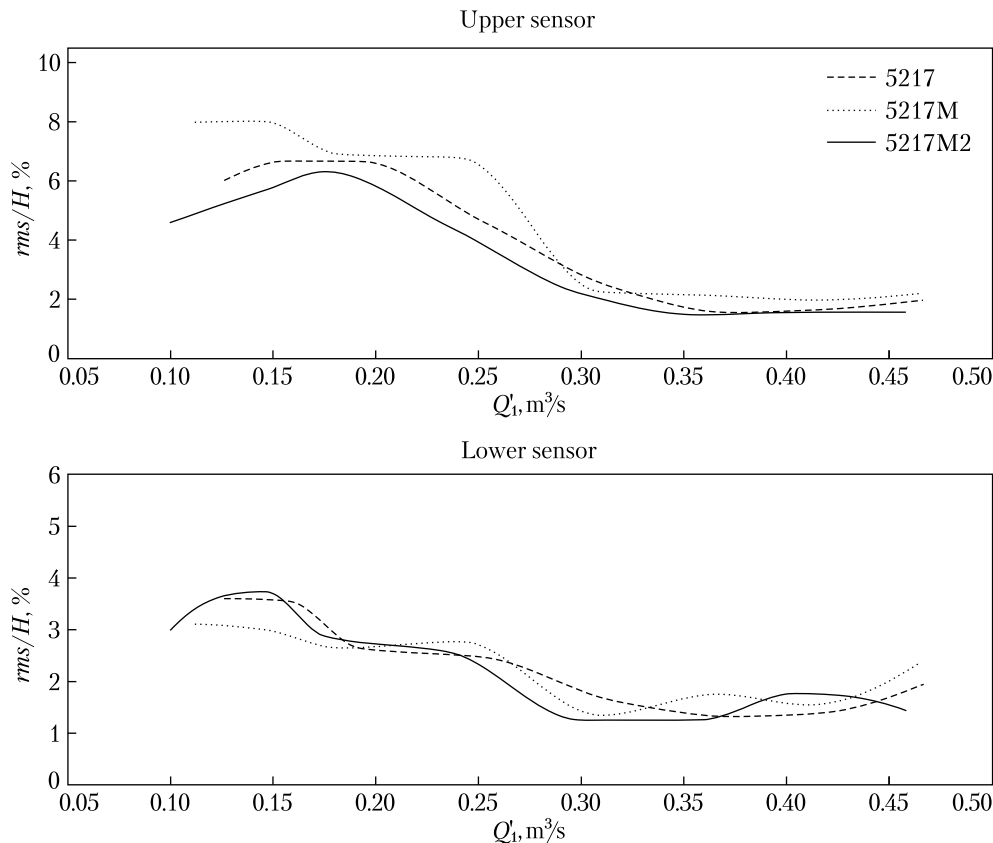
The analysis of the pulsation spectra shown in Fig. 5 shows that at low discharges ( $Q'_1 = 0.252 \text{ m}^3/\text{s}$ ), the maximum values correspond



Fig. 4. Placement of sensors on the draft tube diffuser



**Fig. 5.** Spectra of pressure pulsations in the diffuser for three runners in different modes:  $a - n_1' = 85 \text{ min}^{-1}$ ,  $Q_1' = 0.252 \text{ m}^3/\text{s}$ ;  $b - n_1' = 85 \text{ min}^{-1}$ ,  $Q_1' = 0.467 \text{ m}^3/\text{s}$



**Fig. 6.** Amplitudes of pressure pulsations in the upper and lower parts of the diffuser at the rotation frequency  $n'_1 = 85 \text{ min}^{-1}$

to the vortex rope rotation frequency that is equal to 0.3 of the frequency of runner rotation, and its second harmonic. With an increase in discharge ( $Q'_1 = 0.467 \text{ m}^3/\text{s}$ ), the pulsation amplitudes at frequencies below the frequency of rotation decrease, and the pulsation amplitudes increase at frequencies that are multiples of the frequency of rotation. Thus, in the lower part of the diffuser at discharges up to  $Q'_1 = 0.260 \text{ m}^3/\text{s}$ , a strongly marked pulsation with  $f' = 0.2-0.3$ , which disappears with increasing flow rate. It can also be seen that the maximum values of the pulsation amplitudes in both modes were obtained when studying the RK5217M runner.

At a rotation frequency of  $n'_1 = 85 \text{ min}^{-1}$  that corresponds to the maximum head at the PSP (Fig. 6), the maximum pulsation amplitude  $rms/H$  in the

original version of RK5217 is 6.7%, RK5217M — 7.8%, RK5217M2 — 6.3%. The maximum amplitude of pulsations is observed at discharges up to  $0.180 \text{ m}^3/\text{s}$ , with an increase in discharges up to  $0.360-0.440 \text{ m}^3/\text{s}$ , pulsations decrease to minimum values of 1.5% for RK5217 and RK5217M2, 1.9% for RK5217M.

The maximum amplitude of pulsations  $rms/H$  in the lower part of the diffuser is 3.2–3.8% for all three runners at discharges up to  $0.160 \text{ m}^3/\text{s}$ . As the discharge increases, the pulsations decrease to a minimum value of 1.2–1.8% (at  $Q'_1$  from  $0.300$  to  $0.440 \text{ m}^3/\text{s}$ ). When operating at nominal discharge (95% capacity mode), the pulsation amplitude for the RK5217M runner is 14% higher for the upper sensor and 21% higher for the lower sensor, for the RK5217M2 runner it is 17% lower for the up-

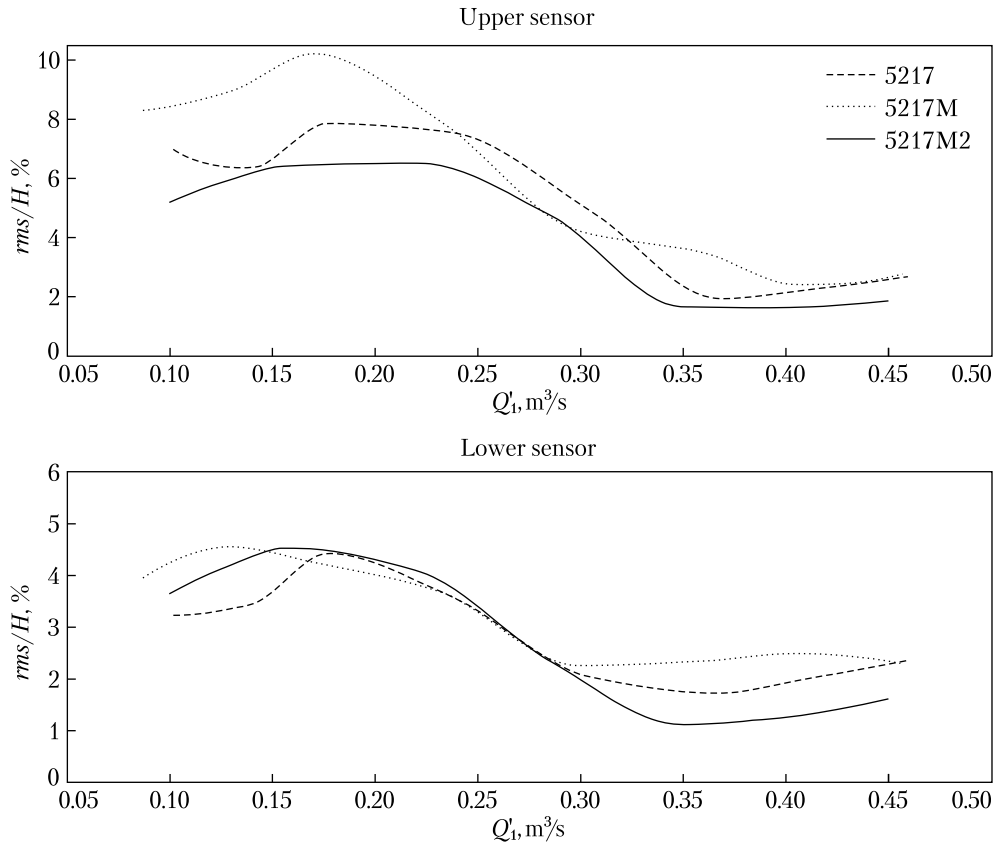


**Fig. 7.** Amplitude of pressure pulsations in the upper and lower parts of the diffuser at the rotation frequency  $n'_1 = 91 \text{ min}^{-1}$

per sensor and 16% lower for the lower sensor; for partial load (50% capacity mode), the pulsation amplitude for the RK5217M runner is 35% higher for the upper sensor and 11% higher for the lower sensor, for the RK5217M2 runner it is 15% lower for the upper sensor and 1% lower for the lower sensor as compared with the RK5217 runner.

For a rotation frequency of  $n'_1 = 91 \text{ min}^{-1}$  that corresponds to the nominal head at the station, the maximum pulsation amplitude  $rms/H$  is observed at discharges up to  $0.200 \text{ m}^3/\text{s}$  (Fig. 7). The maximum values were recorded as follows: RK5217 – 7.9%, RK5217M – 9.2% and 6.5% of RK5217M2. With an increase in the turbine discharge to  $0.350\text{--}0.410 \text{ m}^3/\text{s}$ , the pulsations decrease to a minimum level of 2.0% (RK5217), 2.3% (RK5217M), and 1.8% (RK5217M2).

The maximum amplitude of pulsations  $rms/H$  in the lower part of the diffuser is approximately 4.5% for RK5217 and RK5217M2, 3.8% for RK5217M at discharges up to  $0.180 \text{ m}^3/\text{s}$ . Further, as the discharge increases to  $0.340\text{--}0.380 \text{ m}^3/\text{s}$ , the pulsations decrease to a minimum level of 1.7% (RK5217), 2.2% (RK5217M) and 1.1% (RK5217M2). When operating at nominal discharge (95% capacity mode), the pulsation amplitude for the RK5217M runner is 5% higher for the upper sensor and 1% higher for the lower sensor, and for the RK5217M2 runner it is 28% lower for the upper sensor and 30% lower for the lower sensor; for partial discharge (50% capacity mode), the pulsation amplitude for the RK5217M runner is 2% lower for the upper sensor and 1% lower for the lower sensor, for the RK5217M2

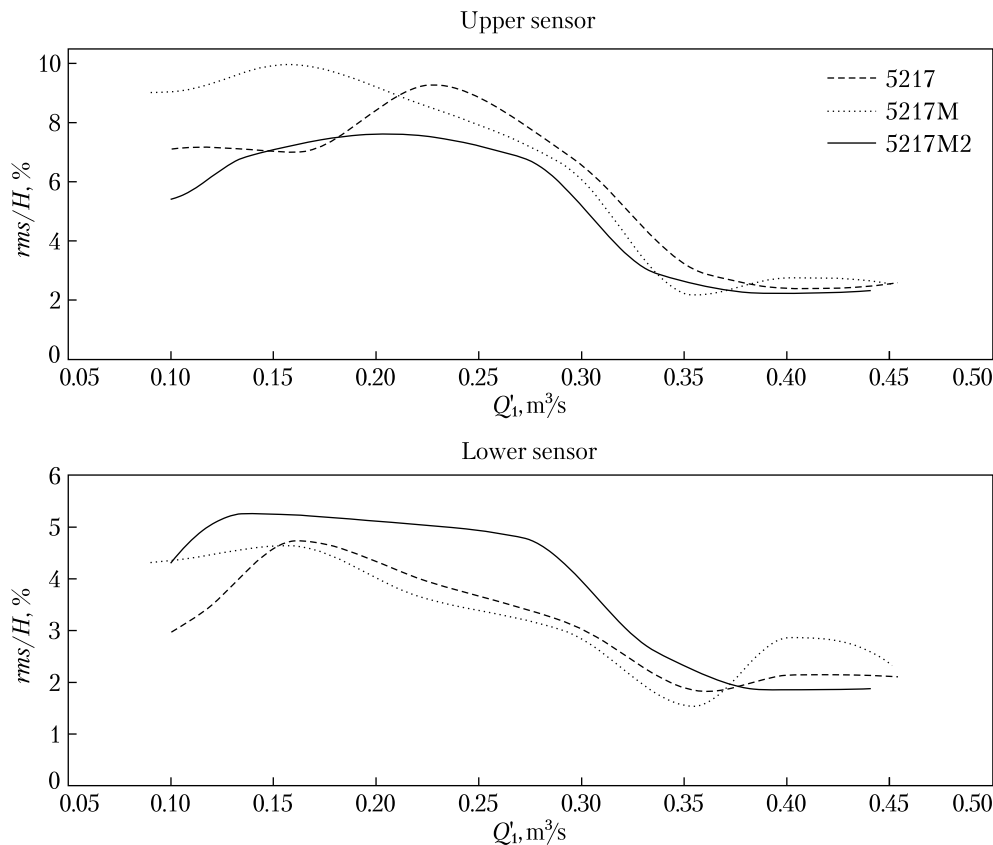


**Fig. 8.** Amplitude of pressure pulsations in the upper and lower parts of the diffuser at the rotation frequency  $n'_1 = 95 \text{ min}^{-1}$

runner it is 19% lower for the upper sensor and 1% lower for the lower sensor as compared with the original RK5217 runner.

For a rotation frequency  $n'_1 = 95 \text{ min}^{-1}$  that corresponds to the minimum head at the station, the maximum pulsation amplitude  $rms/H$  is 9.3% (RK5217), 9.9% (RK5217M), 7.6% (RK5217M2) at discharges up to  $0.250 \text{ m}^3/\text{s}$  (Fig. 8). As the discharge increases, the pulsation amplitude decreases and at a discharge of more than  $0.350 \text{ m}^3/\text{s}$  reaches a minimum value of 2.2–2.4% for all runners.

The maximum amplitude of pulsations  $rms/H$  in the lower part of the diffuser is 4.7% (RK5217), 4.9% (RK5217M) and 5.3% (RK5217M2) at discharges up to  $0.180 \text{ m}^3/\text{s}$ . As the discharge rate increases to  $0.310$ – $0.410 \text{ m}^3/\text{s}$ , the amplitude decreases to 1.8–2.2% (RK5217), 1.4% (RK5217M)

and 0.8–2.4% (RK5217M2). When operating at nominal discharge (95% capacity mode), the pulsation amplitude for the RK5217M runner is 1% less for the upper sensor and 11% more for the lower sensor, for the RK5217M2 runner it is 10% less for the upper sensor and 11% less for the lower sensor, for partial load (50% capacity mode), the pulsation amplitude for the RK5217M runner is 7% smaller for the upper sensor and 7% smaller for the lower sensor, for the RK5217M2 runner it is 14% smaller for the upper sensor and 37% larger for the lower sensor as compared with the original RK5217 runner.

The results show that the flow part with the RK5217M2 runner with a negative circumferential blade lean  $\varphi = -45^\circ$  has the lowest pulsation amplitudes behind the runner (upper sensor) at

all three given rotation speeds for the rated mode (95% capacity) and partial load mode (50% capacity). The maximum decrease in the pulsation amplitude is observed for the RK5217M2 runner in the partial load mode in the upper part of the draft tube diffuser.

In general, almost in the entire range of turbine operating modes for the RK5217M2 runner, a significant decrease in the level of pressure fluctuations in the draft tube diffuser is observed. From the results of selective experimental studies, it was found that the RK5217M2 model has the best characteristics, to confirm which it is proposed to conduct a full range of acceptance tests of a large-scale model with a metal runner with a diameter of 500 mm.

## CONCLUSIONS

1. For pump-turbines for heads up to 200 m, the influence of spatial profiling of runner blades by means of circumferential leans on the energy and pulsation characteristics of the flow part was first established.

2. It has been established that the model of the pump-turbine with RK5217M2 with blades with

a negative circumferential lean  $\varphi = -45^\circ$  in turbine and pump modes has the best energy characteristics among the models of the 5217 series.

3. Thanks to the use of spatial profiling of the runner blades in the pump-turbine model with RK5217M2, it was possible to reduce the level of pressure fluctuations in the draft tube diffuser almost throughout the entire operating range. The maximum reduction of 30% as compared with the original RK5217 runner is observed in the rated load mode (95% of capacity).

## FUNDING OF THE WORK

The scientific work is funded by the National Academy of Sciences of Ukraine under research project “Modeling and research of physical processes in the elements of power machines with the aim of increasing their efficiency and reliability” No. III-5-19 and contract “Development, mathematical and experimental research of the flow parts models of the pump-turbine on the parameters of the Dniester PSP. Conducting acceptance-passing model studies” No. V-23-2022.

## REFERENCES

1. Hydropower capacity should more than double by 2050 to meet climate goals, Irena says. The National News. URL: <https://www.thenationalnews.com/business/energy/2023/02/14/hydropower-capacity-should-more-than-double-by-2050-to-meet-climate-goals-irena-says/> (Last accessed: 03.06.2023).
2. Kougias, I., Aggidis, G., Avellan, F., Deniz, S., Lundin, U., ..., Theodossiou, N. (2019). Analysis of emerging technologies in the hydropower sector. *Renewable and Sustainable Energy Reviews*, 113, 109257. <https://doi.org/10.1016/j.rser.2019.109257>.
3. Zhao, W., Presas, A., Egusquiza, M., Valentín, D., Egusquiza, E., Valero, C. (2021). Increasing the operating range and energy production in Francis turbines by an early detection of the overload instability. *Measurement*, 181, 109580. <https://doi.org/10.1016/j.measurement.2021.109580>.
4. Pasche, S., Avellan, F., Gallaire, F. (2019). Optimal Control of Part Load Vortex Rope in Francis Turbines. *ASME J. Fluids Eng.*, 141(8), 081203. <https://doi.org/10.1115/1.4042560>.
5. Pereira, J. G., Vagnoni, E., Favrel, A., Landry, C., Alligné, S., Nicolet, C., Avellan, F. (2022). Prediction of unstable full load conditions in a Francis turbine prototype. *Mechanical Systems and Signal Processing*, 169, 108666. <https://doi.org/10.1016/j.ymssp.2021.108666>.
6. Pasche, S., Gallaire, F., Avellan, F. (2019). Origin of the synchronous pressure fluctuations in the draft tube of Francis turbines operating at part load conditions. *Journal of Fluids and Structures*, 86, 13–33. <https://doi.org/10.1016/j.jfluidstructs.2019.01.013>.
7. Dörfler, P., Sick, M., Coutu, A. (2013). *Flow-Induced Pulsation and Vibration in Hydroelectric Machinery*. London: Springer-Verlag. <https://doi.org/10.1007/978-1-4471-4252-2>.

8. Lai, X., Chen, X., Liang, Q., Ye, D., Gou, Q., Wang, R., Yan, Y. (2023). Experimental and numerical investigation of vortex flows and pressure fluctuations in a high-head pump-turbine. *Renewable Energy*, 211, 236–247. <https://doi.org/10.1016/j.renene.2023.04.092>.
9. Amini, A., Vagnoni, E., Favrel, A., Yamaishi, K., Müller, A., Avellan, F. (2023). Upper part-load instability in a reduced-scale Francis turbine: an experimental study. *Experiments in Fluids*, 64(6), 110. <https://doi.org/10.1007/s00348-023-03649-0>.
10. Jamali, R., Sohani, A., Hemmatpour, K., Behrang, M., Ghobeity, A. (2022). Experimental study of pressure pulsation in a large-scale hydropower plant with Francis turbine units and a common penstock. *Energy Conversion and Management*, X(16), 100308. <https://doi.org/10.1016/j.ecmx.2022.100308>.
11. Jhankal, N. K., Kumar, A., Mangla, M. (2023). Establishment of correlation for the pressure fluctuations on the low-head Francis turbine in the draft tube cone from the model test. *Flow Measurement and Instrumentation*, 91, 102360. <https://doi.org/10.1016/j.flowmeasinst.2023.102360>.
12. Kumar, S., Cervantes, M. J., Gandhi, B. K. (2021). Rotating vortex rope formation and mitigation in draft tube of hydro turbines – A review from experimental perspective. *Renewable and Sustainable Energy Reviews*, 136, 110354. <https://doi.org/10.1016/j.rser.2020.110354>.
13. Favrel, A., Gomes Pereira Jr, J., Müller, A., Landry, C., Yamamoto, K., Avellan, F. (2020). Swirl number based transposition of flow-induced mechanical stresses from reduced scale to full-size Francis turbine runners. *Journal of Fluids and Structures*, 94, 102956. <https://doi.org/10.1016/j.jfluidstructs.2020.102956>.
14. Favrel, A., Liu, Z., Hossein Khozaei, M., Irie, T., Miyagawa, K. (2022). Anti-phase oscillations of an elliptical cavitation vortex in Francis turbine draft tube. *Physics of Fluids*, 34, 064112. <https://doi.org/10.1063/5.0091210>.
15. Hossein Khozaei, M., Favrel, A., Miyagawa, K. (2022). Influence of swirling flow parameters on frequency response of a simplified draft-tube in presence of cavitation. *International Journal of Heat and Fluid Flow*, 98, 109043. <https://doi.org/10.1016/j.ijheatfluidflow.2022.109043>.
16. Shahzer, M. A., Cho, Y., Shamsuddeen, M. M., Kim, J.-H. (2023). Investigation of cavitating vortex rope instabilities and its suppression inside a Francis turbine model with Thoma number variation. *Physics of Fluids*, 35(3), 033310. <https://doi.org/10.1063/5.0140973>.
17. Muhirwa, A., Li, B., Su, W.-T., Liu, Q.-Z., Binama, M., Wu, J., Cai, W.-H. (2020). Investigation on mutual traveling influences between the draft tube and upstream components of a Francis turbine unit. *Renewable Energy*, 162, 973–992. <https://doi.org/10.1016/j.renene.2020.08.107>.
18. Geng, C., Li, Y., Tsujimoto, Y., Nishi, M., Luo, X. (2022). Pressure oscillations with ultra-low frequency induced by vortical flow inside Francis turbine draft tubes. *Sustainable Energy Technologies and Assessments*, 51, 101908. <https://doi.org/10.1016/j.seta.2021.101908>.
19. Liu, Z., Favrel, A., Takahashi, W., Miyagawa, K. (2021). Numerical simulation of the unsteady cavitating flow in a Francis turbine draft tube at Upper-Part-Load (UPL) conditions. *IOP Conference Series: Earth and Environmental Science*, 774, 012089. <https://doi.org/10.1088/1755-1315/774/1/012089>.
20. Khullar, S., Kumar, S., Singh, K. M., Cervantes, M. J., Gandhi, B. K. (2021). Influence of the runner cone design on the pressure fluctuations in the draft tube of a low head Francis turbine. *IOP Conference Series: Earth and Environmental Science*, 774, 012110. <https://doi.org/10.1088/1755-1315/774/1/012110>.
21. Wang, L., Cui, J., Shu, L., Jiang, D., Xiang, C., Li, L., Zhou, P. (2022). Research on the Vortex Rope Control Techniques in Draft Tube of Francis Turbines. *Energies*, 15(24), 9280. <https://doi.org/10.3390/en15249280>.
22. Grein, H. (1981). Vibration phenomena in Francis turbines: their causes and prevention. *Escher Wyss News*, 54, 37–42.
23. Joy, J., Rasee, M., Cervantes, M. J. (2023). Experimental investigation of an adjustable guide vane system in a Francis turbine draft tube at part load operation. *Renewable Energy*, 210, 737–750. <https://doi.org/10.1016/j.renene.2023.04.096>.
24. Zhou, X., Wu, H., Shi, C. (2019). Numerical and experimental investigation of the effect of baffles on flow instabilities in a Francis turbine draft tube under partial load conditions. *Advances in Mechanical Engineering*, 11(1), 1687814018824468. <https://doi.org/10.1177/1687814018824468>.
25. Bucur, D. M., Dunca, G., Bunea, F., Ciocan, G. D. (2019). Experimental analysis of the operation of a small Francis turbine equipped with an innovative aeration device. *IOP Conference Series: Earth and Environmental Science*, 240(4), 042010. <https://dx.doi.org/10.1088/1755-1315/240/4/042010>.
26. Khullar, S., Singh, K. M., Cervantes, M. J., Gandhi, B. K. (2022). Numerical Analysis of Water Jet Injection in the Draft Tube of a Francis Turbine at Part Load Operations. *ASME. J. Fluids Eng.*, 144(11), 111201. <https://doi.org/10.1115/1.4054564>.
27. Mohammadi, M., Hajidavalloo, E., Behbahani-Nejad, M. (2019). Investigation on Combined Air and Water Injection in Francis Turbine Draft Tube to Reduce Vortex Rope Effects. *ASME. J. Fluids Eng.*, 141(5), 051301. <https://doi.org/10.1115/1.4041565>.

28. Zhou, X., Wu, H., Cheng, L., Huang, Q., Shi, C. (2023). A new draft tube shape optimisation methodology of introducing inclined conical diffuser in hydraulic turbine. *Energy*, 265, 126374. <https://doi.org/10.1016/j.energy.2022.126374>.
29. Su, W.-T., Binama, M., Li, Y., Zhao, Y. (2020). Study on the method of reducing the pressure fluctuation of hydraulic turbine by optimizing the draft tube pressure distribution. *Renewable Energy*, 162, 550–560. <https://doi.org/10.1016/j.renene.2020.08.057>.
30. Chen, Z., Baek, S.-H., Cho, H., Choi, Y.-D. (2019). Optimal design of J-groove shape on the suppression of unsteady flow in the Francis turbine draft tube. *Journal of Mechanical Science and Technology*, 33(5), 2211–2218. <https://doi.org/10.1007/s12206-019-0423-x>.
31. Lai, X.-D., Liang, Q.-W., Ye, D.-X., Chen, X.-M., Xia, M.-M. (2019). Experimental investigation of flows inside draft tube of a high-head pump-turbine. *Renewable Energy*, 133, 731–742. <https://doi.org/10.1016/j.renene.2018.10.058>.
32. Zhang, F., Xiao, R., Zhu, D., Liu, W., Tao, R. (2023). Pressure pulsation reduction in the draft tube of pump turbine in turbine mode based on optimization design of runner blade trailing edge profile. *Journal of Energy Storage*, 59, 106541. <https://doi.org/10.1016/j.est.2022.106541>.
33. Lampart, P., Rusanov, A., Yershov, S., Marcinkowski, S., Gardzilewicz, A. (2005). Validation of a 3D RANS solver with a state equation of thermally perfect and calorically imperfect gas on a multi-stage low-pressure steam turbine flow. *Journal of Fluids Engineering*, 127(1), 83–93. <https://doi.org/10.1115/1.1852491>.
34. Rusanov, A. V., Subotin, V. H., Khoryev, O. M., Bykov, Y. A., Korotaiev, P. O., Ahibalov, Y. S. (2022). Effect of 3D Shape of Pump-Turbine Runner Blade on Flow Characteristics in Turbine Mode. *J. of Mech. Eng.*, 25(4), 6–13. <https://doi.org/10.15407/pmach2022.04.006>.
35. Lampart, P., Gardzilewicz, A., Yershov, S., Rusanov, A. (2001). Investigation of interaction of the main flow with root and tip leakage flows in an axial turbine stage by means of a source/sink approach for a 3D Navier-Stokes solver. *Journal of Thermal Science*, 10(3), 198–204. <https://dx.doi.org/10.1007/s11630-001-0019-4>.
36. Lampart, P., Gardzilewicz, A., Rusanov, A., Yershov, S. (1999). The effect of stator blade compound lean and compound twist on flow characteristics of a turbine stage – Numerical study based on 3D NS simulations. *American Society of Mechanical Engineers, Pressure Vessels and Piping Division PVP*, 397(II), 195–204.
37. Yershov, S., Rusanov, A., Gardzilewicz, A., Lampart, P. (1999, August). Calculations of 3D viscous compressible turbomachinery flows. *Proc. 2<sup>nd</sup> Symp. on Comp. Technologies for Fluid/ Thermal/Chemical Systems with Industrial Applications, ASME PVP Division Conf. (1–5 August, 1999, Boston, USA)*, 397.2, 143–154.
38. Rusanov, A. V., Solovey, V. V., Lototsky, M. V. (2020). Thermodynamic features of metal hydride thermal sorption compressors and perspectives of their application in hydrogen liquefaction systems. *Journal of Physics: Energy*, 2(2), 021007. <https://doi.org/10.1088/2515-7655/ab7bf4>.
39. Bykov, Y., Khoryev, O., Korotaiev, P., Dedkov, V., Agibalov, Y. (2022, October). Numerical Investigation of Unsteady Flow in Draft Tube with Ribs. *2022 IEEE KhPI Week on Advanced Technology (KhPIWeek) (3–7 Oct. 2022, Kharkiv)*, 589–594. <https://doi.org/10.1109/KhPIWeek57572.2022.9916461>.
40. Khoryev, O., Korotaiev, P., Agibalov, Y., Bykov, Y., Maksymenko-Sheiko, K. (2023). Experimental Studies of Pump-Turbine Flow Part Models at Heads of 80–120 m. In *Advances in Mechanical and Power Engineering. CAMPE 2021. Lecture Notes in Mechanical Engineering*. Cham: Springer. 24–33. [https://doi.org/10.1007/978-3-031-18487-1\\_3](https://doi.org/10.1007/978-3-031-18487-1_3)

Received 15.07.2023

Revised 16.10.2023

Accepted 23.11.2023

А.В. Русанов<sup>1</sup> (<https://orcid.org/0000-0002-9957-8974>),  
В.Г. Суботин<sup>2</sup> (<https://orcid.org/0000-0002-2489-5836>),  
О.М. Хорев<sup>1</sup> (<https://orcid.org/0000-0001-6940-4183>),  
О.В. Линник<sup>2</sup> (<https://orcid.org/0000-0003-1946-3032>),  
Ю.А. Биков<sup>1</sup> (<https://orcid.org/0000-0001-7089-8993>),  
П.О. Коротаєв<sup>1</sup> (<https://orcid.org/0000-0002-7473-9508>),  
Є.С. Агібалов<sup>1</sup> (<https://orcid.org/0000-0003-3866-9992>)

<sup>1</sup> Інститут проблем машинобудування ім. А.М. Підгорного Національної академії наук України,  
вул. Пожарського, 2/10, Харків, 61046, Україна,  
+380 57 349 4724, [admi@ipmach.kharkov.ua](mailto:admi@ipmach.kharkov.ua)

<sup>2</sup> АТ «Українські енергетичні машини»,  
просп. Героїв Харкова, 199, Харків, 61037, Україна,  
+380 57 349 2171, [office@ukrenergymachines.com](mailto:office@ukrenergymachines.com)

## ЕКСПЕРИМЕНТАЛЬНІ ДОСЛІДЖЕННЯ ПУЛЬСАЦІЙ ТИСКУ В ДИFUЗОРІ ВІДСМОКТУВАЛЬНОЇ ТРУБИ У МОДЕЛЯХ НАСОС-ТУРБІНИ НА НАПОРИ ДО 200 м

**Вступ.** Збільшення частки маневрових і резервних генеруючих потужностей для покриття добових піків споживання електроенергії є одним із першочергових завдань повоєнного розвитку енергетики України.

**Проблематика.** На сьогодні до гідротурбін висувають вимоги не тільки з підвищення ефективності, а й із розширення діапазону роботи. Так, нові гідроагрегати Дністровської ГАЕС мають забезпечити надійну експлуатацію в турбінному режимі у діапазоні потужностей 40—100 % від номінальної, тоді як чотири раніше встановлені працюють у діапазоні 70—100 %. Виконати це можливо за рахунок підвищення ККД і зниження рівня пульсацій тиску на режимах малих потужностей.

**Мета.** Встановити закономірності розподілу пульсацій тиску в дифузорі відсмоктувальної труби моделі гідроагрегату на основі дослідження впливу просторової форми лопатей робочих коліс радіально-осьової насос-турбіни на гідродинамічний процес у проточній частині.

**Матеріали й методи.** Селективні експериментальні дослідження трьох варіантів моделей проведено на гідродинамічному стенді ІПМаш ЕКС-30. Лопаті робочих коліс виготовлено з пластику *PLA* методом 3D-друку, що дозволило скоротити строки досліджень і знизити витрати. Пульсації тиску вимірювали датчиками у двох точках дифузору відсмоктувальної труби на відстані 0,2 і 1,5 діаметра робочого колеса від обода колеса.

**Результати.** За допомогою колових навалів спроектовано й експериментально досліджено три модифікації робочого колеса насос-турбіни на напори до 200 м, що відрізнялися лише взаємним розташуванням профілів лопатей. Аналіз отриманих універсальних енергетичних і пульсаційних характеристик моделей у турбінному режимі показав, що кращі показники має модель із робочим колесом із негативним коловим навалом лопатей.

**Висновки.** Визначений вплив просторової форми лопатей робочих коліс на енергетичні й пульсаційні характеристики моделі радіально-осьової насос-турбіни на напори до 200 м дозволив підвищити її ефективність і знизити рівень пульсацій тиску у проточній частині.

**Ключові слова:** насос-турбіна, проточна частина, пульсації тиску, робоче колесо, відсмоктувальна труба, експериментальні дослідження.